# Automated position and size selection of round applicators for AccuBoost breast brachytherapy


F. L. West[1,2], R. Munbodh[2,3], M. J. Rivard[2,3], J. C. Patrick[2,3] , S. A. Roles[1,2] J. T. Hepel[2,3], K. L. Leonard[2,3], D. E. Wazer[2,3], Z. H. Saleh[2,3]

1 University of Rhode Island, Kingston, Rhode Island

2 Rhode Island Hospital, Providence, Rhode Island

3 Warren Alpert Medical School of Brown University, Providence, Rhode Island


BROWN Alpert Medical School

UNIVERSITY OF RHODE ISLAND · HOPE · 1892


JULY 12–16 2020 VIRTUAL JOINT AAPM | COMP MEETING EASTERN TIME [GMT-4]

Improving Health QUALITY, Increasing Global IMPACT


## INTRODUCTION

AccuBoost is a complex non-invasive breast treatment using high-dose-rate (HDR) brachytherapy [1,2] and a set of specially designed applicators with different shapes, round or D-shaped, and different sizes that are connected to an HDR $^{192}$Ir remote afterloader. A patient's breast is first immobilized between compression paddles with moderate compression so a mammographic image can be taken [3]. The image is used to localize the lumpectomy cavity and surgical clips left in the margins of the tumor bed during lumpectomy. The radiation oncologist will then overlay physical transparencies to visually select the applicator type, position and size based upon the specific disease, position of the tumor bed, excised tumor pathology, compressed breast thickness, position of surgical clips, and texture in the breast tissue.

## AIM

Improve uniformity in determining the applicator location and size and reduce the duration of patient compression. An algorithm was created in MATLAB™ (version 2019b, Mathworks, Natick, MA) that automates the selection of round AccuBoost applicators based on positions of surgical clips.

## METHODS

Ten patients treated with AccuBoost were retrospectively selected from our patient database. A total of 42 fractions were analyzed and were treated with a round applicator and were imaged with a standard procedure.

Mammographic images used for treatment planning were 23.4 cm X 18.8 cm with a spatial resolution of 145 pixels per cm. The ImageJ (NIH, LOCI, University of Wisconsin, Madison, WI) anonymization plugin was used to remove all patient identifiers. An example of the raw image can be seen in Fig. 1a.

Templates of the A and O position markers were acquired from a blank image of the imprinted grid. A normalized 2D cross correlation function was used with the A and O templates to localize regions in the image with the highest correlation. The grid points above the A and O markers were found and used as reference points to localize the rest of the grid.

A mask was created for gridlines and non-treatable regions to remove areas where surgical clips would not be found. A threshold of TH = 0.935 x (maximum intensity) was applied to preserve pixels corresponding to clips and some other (grid markers, high-density tissue, etc.) undesired regions. An image after this step can be seen in Fig. 1b. The image was binarized and pixels were grouped into regions. Any regions not corresponding to clips (small area, high Euler number, low eccentricity and circularity) were removed (Fig. 1c). A series of morphological operations were then applied to dilate, fill, smooth, and erode the regions to reform their original shape (Fig. 1d).

The remaining regions were manually labeled as clip or non-clip and the region properties (area, perimeter, area/perimeter ratio, eccentricity, circularity, eccentricity/circularity ratio, major axis length, minor axis length, axis length ratio, mean pixel value, minimum pixel value, range of pixel values and standard deviation of pixel values) were extracted. A total of 946 regions from 42 fractions with 191 regions corresponding to clips and 755 regions corresponding to non-clip regions. These regions were used to train a support vector machine (SVM) model in the Classification Learner in MATLAB to determine if regions were a clip. The model was optimized over 50 iterations and used a five-fold cross-validation to prevent overfitting of the training data.

The applicator position was calculated with the center-of-mass of identified clips in the x (lateral) and y (anterio-posterior) directions. The position was then shifted to the nearest 0.5-cm step-size on the grid based on the precision of applicator positioning at our institution. The applicator size was defined by the diameter of the tumor bed (delineated by surgical clips) plus a 1-cm isotropic margin [4]. This size was then rounded to nearest 1-cm, which represents the available applicator sizes. Fig. 2 show an image with the identified clips (green outlines with red enumerations), algorithm-predicted applicator and center (cyan circle and fuchsia crosshair), and a display that conveniently presents these parameters.

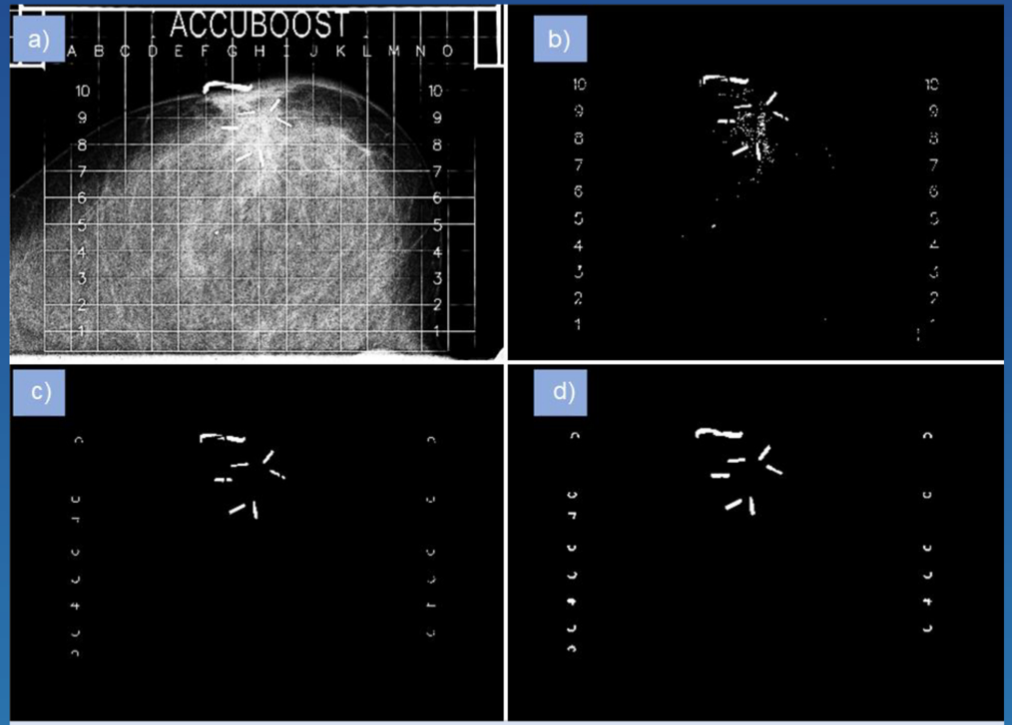


**Figure 1.** a) Mammographic image before processing b) gridlines and non-treatable regions masked out with a threshold applied c) regions with properties corresponding to tissue (small area, high Euler number, and low eccentricity and circularity) removed d) remaining regions undergo morphological operations to reform to original shape.

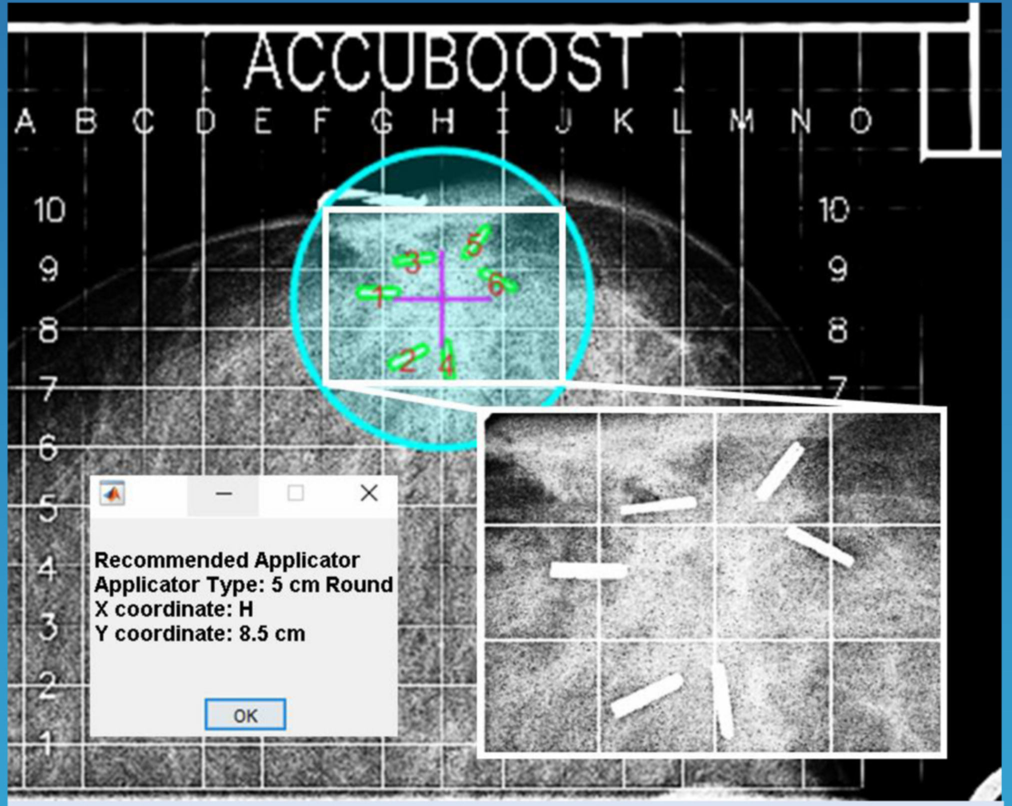


**Figure 2.** Algorithm displayed original image with regions identified as clips (green outline with red enumerations), algorithm-predicted center (fuchsia crosshair), and predicted applicator (cyan circle). The clips from the raw image are shown (inset) to visualize the detected region. A display also appears to indicate the predicted coordinates and size for the user's convenience.

## RESULTS

**Surgical Clip Detection**

Of 946 regions, 192 were classified as clips (true positive = 185, false positive = 7) and 754 were classified as miscellaneous regions (true negative = 748, false negative = 6). This resulted in a sensitivity of 96.9% and specificity of 99.1% for regions representing clips being correctly detected. In 30 of 42 treatment fractions, all the surgical clips were correctly identified. An additional 6 of 42 fractions had no misidentified regions, but were missing some of the clips.

**Predicted Applicator Position**

Distances between the physician-selected and algorithm-predicted applicator center positions are shown in Fig. 3. The applicator position was correctly predicted for 20 of 42 fractions and was within 0.5 cm for 33 of 42 fractions. Maximum difference in positions was 1.12 cm. Maximum differences between any x or y coordinates were ≤ 1.0 cm.

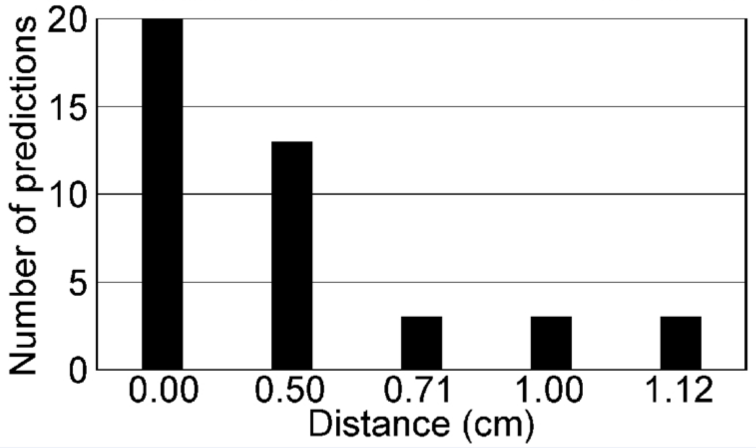


**Figure 3.** Distance between the physician-selected and algorithm-predicted applicator center positions for the 42 fractions. Since the applicator could only be placed with 0.5 cm precision, the total distances between the physician-selected and algorithm-predicted applicator center positions had discrete values.

**Table 1.** A confusion matrix comparing the physician-selected and algorithm-predicted applicator sizes for the 42 fractions. The diagonal was bolded to signify that those were cases when selected/predicted sizes were the same.

| Applicator size (cm) | | Algorithm-predicted | | | |
|---|---|---|---|---|---|
| | | 5 | 6 | 7 | 8 |
| Physician-selected | 5 | **10** | 4 | 0 | 0 |
| | 6 | 7 | **8** | 3 | 0 |
| | 7 | 0 | 0 | **4** | 3 |
| | 8 | 0 | 0 | 0 | **3** |

Applicator size was correctly predicted for 25 of 42 fractions (Table 1), with maximum discrepancy ≤ 1 cm for the remaining 17 fractions. Since applicators are available in 5, 6, 7, and 8 cm diameters, corresponding calculated diameters ranged from 4.88 to 6.37 cm, 4.93 to 7.05 cm, 6.86 to 8.24 cm, and 8.86 to 9.33 cm, respectively. Both applicator position and size were correctly predicted (no difference) for 13 of 42 fractions (31.7%). Size was predicted correctly with position differing by 0.5 cm for 8 of 42 cases. Position was predicted correctly with applicator size differing by 1 cm for 7 of the 42 fractions. These made up 28 of 42 fractions (66.7%) where the algorithm-predicted applicator differed by at most the smallest increment in either position or size.

## CONCLUSIONS

The described algorithm both automatically and consistently selects the position and size of round AccuBoost applicators based on imaging of surgical clips. Selection accuracy is less than 95% when compared to physician-selected parameters and is not adequate to be considered as the primary determinant of treatment decision in the clinic. Standalone capabilities require further work to implement radiomic feature detection and consider inter-physician variability.

The algorithm shows promise for some applications in the clinic. The clip detection model in the algorithm has a high sensitivity (96.9%) and high specificity (99.1%) which can provide helpful information to the radiation oncologist to simplify their decision. This consequently could also lead to uniform and quicker decisions by the radiation oncologists. The algorithm could also be applied as an independent check to physician-selected parameters. Most predictions (66.7%) were within the smallest increment of deviation in either position or size, and thusly could be used to identify large deviations to ensure that treatment decisions are consistent to the quantitative data extracted from the image.

## CONTACT INFORMATION


Email: west.foster96@gmail.com.


## ACKNOWLEDGEMENTS


The authors express their gratitude to Dr. Yana Reshetnyak at the University of Rhode Island for her oversight of this study, and to Raymond Bricault Jr. at Advanced Radiation Therapy, LLC (Tewksbury, MA) for constructive comments and insight on the AccuBoost process. Drs. Rivard and Wazer are minor shareholders of Advanced Radiation Therapy, the manufacturer of the AccuBoost breast brachytherapy unit.


## REFERENCES


1. Rivard et al. Dosimetric characterization of round HDR $^{192}$Ir AccuBoost applicators for breast brachytherapy. *Med Phys* 2009; 33: 5027-5032.

2. Yang et al. Dosimetric optimization of a conical breast brachytherapy applicator for improved skin-dose sparing. *Med Phys* 2010; 37: 5665-5671.

3. Hepel et al. Factors influencing eligibility for breast boost using noninvasive image-guided breast brachytherapy. *Brachytherapy* 2014; 13: 579-583.

4. Leonard et al. Prescription dose evaluation for APBI with noninvasive image-guided breast brachytherapy using equivalent uniform dose. *Brachytherapy* 2015; 14: 496-501.